Theoretical Insights on the Interaction of Uranium with Amidoxime and Carboxyl Groups

8 AUTHORS, INCLUDING:

Jian Hui Lan
Chinese Academy of Sciences
53 PUBLICATIONS **1,419** CITATIONS

SEE PROFILE

Xiangke Wang
Chinese Academy of Sciences
307 PUBLICATIONS **13,398** CITATIONS

SEE PROFILE

Wei-Qun Shi
Chinese Academy of Sciences
70 PUBLICATIONS **502** CITATIONS

SEE PROFILE

Theoretical Insights on the Interaction of Uranium with Amidoxime and Carboxyl Groups

Cong-Zhi Wang,[†] Jian-Hui Lan,[†] Qun-Yan Wu,[†] Qiong Luo,[‡] Yu-Liang Zhao,[†] Xiang-Ke Wang,[§] Zhi-Fang Chai,[*,†,∥] and Wei-Qun Shi[*,†]

[†]Group of Nuclear Energy Chemistry, Key Laboratory of Nuclear Radiation and Nuclear Energy Technology and Key Laboratory for Biomedical Effects of Nanomaterials and Nanosafety, Institute of High Energy Physics, Chinese Academy of Sciences, Beijing 100049, China

[‡]MOE Key Laboratory of Theoretical Environmental Chemistry, Center for Computational Quantum Chemistry, South China Normal University, Guangzhou 510631, China

[§]Key Laboratory of Novel Thin Film Solar Cells, Institute of Plasma Physics, Chinese Academy of Sciences, Hefei 230031, China

[∥]School for Radiological and Interdisciplinary Sciences (RAD-X) and Collaborative Innovation Center of Radiation Medicine of Jiangsu Higher Education Institutions, Soochow University, Suzhou 215123, China

S *Supporting Information*

ABSTRACT: Recovery of uranium from seawater is extremely challenging but important for the persistent development of nuclear energy, and thus exploring the coordination structures and bonding nature of uranyl complexes becomes essential for designing highly efficient uranium adsorbents. In this work, the interactions of uranium and a series of adsorbents with various well-known functional groups including amidoximate (AO^-), carboxyl (Ac^-), glutarimidedioximate (HA^-), and bifunctional AO^-/Ac^-, HA^-/Ac^- on different alkyl chains ($R'=CH_3$, $R''=C_{13}H_{26}$) were systematically studied by quantum chemical calculations. For all the uranyl complexes, the monodentate and η^2 coordination are the main binding modes for the AO^- groups, while Ac^- groups act as monodentate and bidentate ligands. Amidoximes can also form cyclic imide dioximes (H_2A), which coordinate to UO_2^{2+} as tridentate ligands. Kinetic analysis of the model displacement reaction confirms the rate-determining step in the extraction process, that is, the complexing of uranyl by amidoxime group coupled with the dissociation of the carbonate group from the uranyl tricarbonate complex $[UO_2(CO_3)_3]^{4-}$. Complexing species with AO^- groups show higher binding energies than the analogues with Ac^- groups. However, the obtained uranyl complexes with Ac^- seem to be more favorable according to reactions with $[UO_2(CO_3)_3]^{4-}$ as reactant, which may be due to the higher stability of HAO compared to HAc. This is also the reason that species with mixed functional group AO^-/Ac^- are more stable than those with monoligand. Thus, as reported in the literature, the adsorbability of uranium can be improved by the synergistic effects of amidoxime and carboxyl groups.
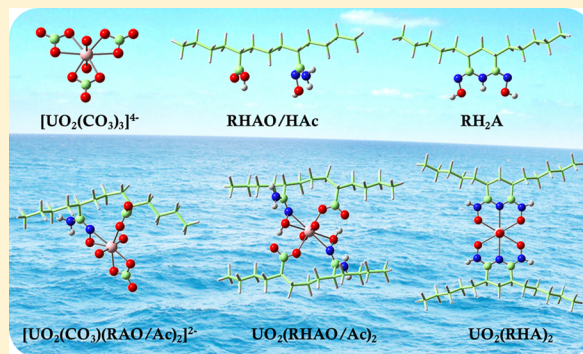
1. INTRODUCTION

Uranium sources are vital for nuclear energy production. It has been reported that there are approximately 4 billion tons of uranium in seawater, which is 1000 times higher than that available in terrestrial ores.[1] Thus, seawater is considered to be an inexhaustible source of uranium. However, adsorption of uranium from seawater is challenging because in seawater uranium mainly exists in the stable carbonate complexes of $[UO_2(CO_3)_3]^{4-}$ with a very low concentration of about 3.3 μg/ L.[2,3] Besides, the large amount of competing metal ions, such as sodium, potassium, calcium, and some transition metal ions, is another major obstacle to efficient extraction of uranium.[1−4]

Recovery of uranium from seawater has been extensively studied over several decades. It has been found that amidoxime-based adsorbents show high tendency toward uranium.[5−12]

Figure 1 shows the possible binding modes for amidoxime chelation to uranyl, that is, the monodentate coordination with the oxime oxygen atom (Figure 1a), the coordination through the oxime oxygen and the amine nitrogen atoms forming five-membered chelate rings (Figure 1b), and the η^2 coordination via the N−O bond (Figure 1c). Recently, Vukovic et al.[13] studied a series of uranyl complexes with acetamidoximate and aqua ligands by single-crystal X-ray diffraction and density functional theory (DFT) calculations. They found that the η^2 mode is the most stable form for uranyl complexes. Additionally, some investigations[14−16] also indicated that amidoximes can form cyclic imide dioximes, which can coordinate to uranyl cation as
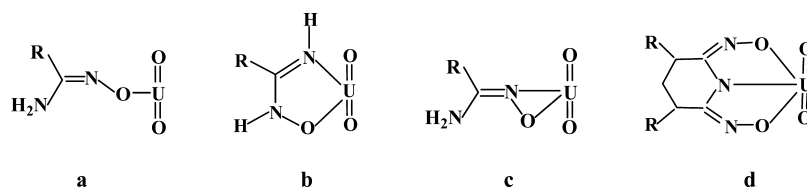
Figure 1. Possible binding modes for the amidoxime group coordination to uranyl ions.

$[UO_2(CO_3)_2(R'AO)]^{3-}$ $[UO_2(CO_3)(H_2O)(R'AO)_2]^{2-}$ $[UO_2(R'AO)_3]^-$ $[UO_2(CO_3)_2(R'Ac)]^{3-}$ $[UO_2(CO_3)(H_2O)(R'Ac)_2]^{2-}$

$[UO_2(R'Ac)_3]^-$ $[UO_2(CO_3)(H_2O)(R'AO)(R'Ac)]^{2-}$ $UO_2(H_2O)_2(R'AO)(R'Ac)$ $[UO_2(R'AO)_2(R'Ac)]^-$ $[UO_2(R'AO)(R'Ac)_2]^-$

$[UO_2(H_2O)(R'_2HA)(CO_3)]^-$ $[UO_2(H_2O)_3(R'_2HA)]^+$ $UO_2 (R'_2HA)_2$ $UO_2(H_2O)(R'_2HA)(R'Ac)$
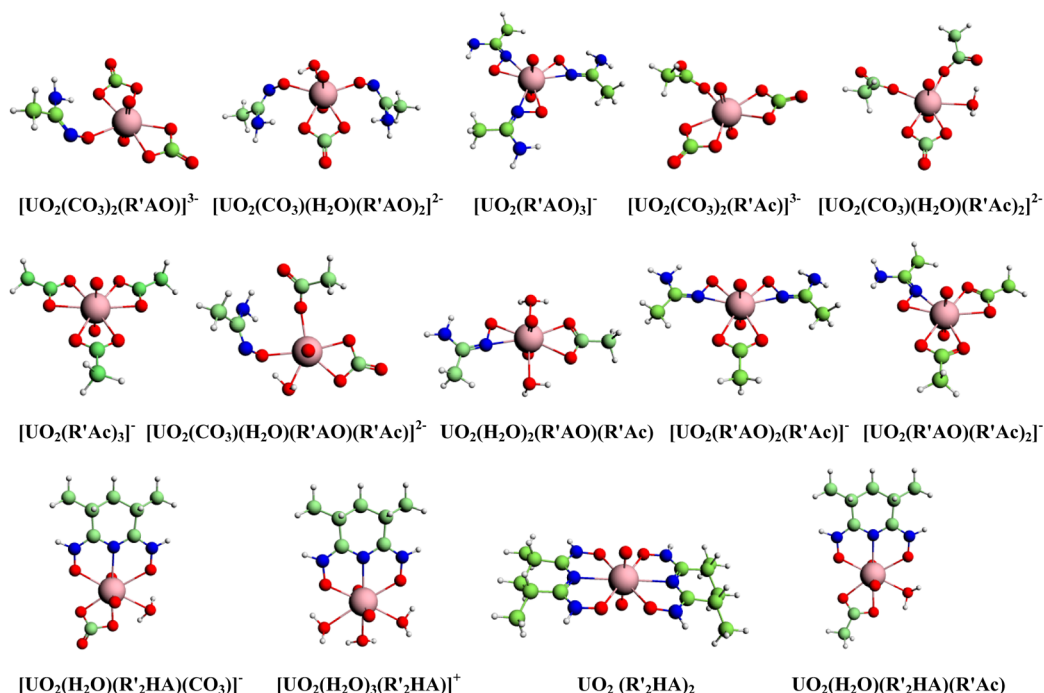
Figure 2. Optimized structures of uranyl complexes with $R'AO^-$, $R'Ac^-$, R'_2HA^- (R'=CH_3), and CO_3^{2-} by the B3LYP method. The subsequent figures adopt the same arrangement.

tridentate ligands (Figure 1d) and seem to be more effective for complexing UO_2^{2+}.

Although adsorbents with amidoxime groups have some advantages in the application of uranium recovery from seawater, improving the uranium adsorption rate is still a major challenge.[17] In uranium adsorption, the dissociation of $[UO_2(CO_3)_3]^{4-}$ is probably the rate-determining step.[18,19] Previous studies[20−22] discovered that the introduction of hydrophilic groups such as carboxyl groups can increase the U(VI)-uptake efficiency, which may be due to the hydrogen ions from the carboxyl groups promoting the decomplexation of the uranyl tricarbonate complexes. Choi and Nho[23] prepared the polyethylene adsorbents containing amidoxime, carboxyl, and amidoxime/carboxyl groups. With the ratio of amidoxime/carboxyl (50/50 mol %), the polyethylene adsorbents show the maximum adsorption of uranyl ions. Using Fourier transform infrared (FTIR) spectroscopy, they found that amidoxime and carboxyl groups on polyethylene adsorbents can act as monodentate ligands to the uranyl ions. Furthermore, it has been demonstrated that seawater temperature affects the chemical adsorption of uranium, and extraction efficiency can be improved in warmer seawaters.[24]

So far, many experimental investigations on uranium recovery from seawater by adsorbents with amidoxime and some acidic groups have been reported.[5−16,20−22] Recently, computational chemistry has been applied to study the issue of uranium complexation in seawater at the molecular level. However, as far

as we know, the published theoretical works[13,16,25−27] only focused on materials with one kind of functional group such as amidoxime or acidic ligands used in uranium extraction. In the present work, we aim to explore the synergistic effect of the amidoxime and acidic groups, the coordination modes of these functional groups, and the interaction mechanisms of uranium extraction. A series of adsorbents with amidoximate (AO⁻), carboxyl (Ac⁻), and amidoximate/carboxyl (AO⁻/Ac⁻) for uranium sequestration were studied in detail by quantum chemical calculations.

2. THEORETICAL METHODS

All calculations were implemented in the Gaussian 09 program[28] by using the DFT method[29−32] with the B3LYP[33,34] hybrid functional. Scalar relativistic calculations were performed without considering spin−orbit coupling effects. The quasi-relativistic effective core potentials (RECP) replacing 60 core electrons for actinides and the corresponding valence basis sets[35−37] were used for uranium. The 6-311G(d, p) basis sets were adopted for hydrogen, carbon, nitrogen, and oxygen atoms. Our previous studies[38−42] confirmed that this level of theory can get accurate geometries and energetics for actinide species. Besides, geometry optimizations were carried out with no symmetry restrictions. At the B3LYP/6-311G(d, p)/RECP level of theory, vibrational frequency analyses were performed to verify the minima character of the optimized structures.

On the basis of optimized molecules in the gas phase, solvent effects of water were modeled at the same level of theory by the conductor-like polarizable continuum model (CPCM),[43−46] which is similar to the conductor-like screening model (COSMO),[43] with the Klamt atomic

Table 1. U−N and U−O Average Bond Lengths (Å) for the Uranyl Complexes with R′AO⁻, R′Ac⁻, R′₂HA⁻, CO₃²⁻, and the Symmetrical and Antisymmetrical Stretching Frequency (v_s and v_{as}, cm⁻¹) of U=O(axial) Calculated by the B3LYP Method

species	U=O (axial)	U−N (R′AO⁻/R′₂HA⁻)	U−O (R′AO⁻/R′₂HA⁻)	U−O (R′Ac⁻)	U−O (CO₃²⁻)	U−O (H₂O)	v_s	v_{as}
[UO₂(CO₃)₃]⁴⁻	1.833				2.527		754	824
[UO₂(CO₃)₂(R′AO)]³⁻	1.824		2.364		2.428		778	843
[UO₂(CO₃)(H₂O)(R′AO)₂]²⁻	1.814		2.311		2.368	2.953	792	876
[UO₂(R′AO)₃]⁻	1.803	2.472	2.381				813	894
[UO₂(CO₃)₂(R′Ac)]³⁻	1.821			2.490	2.406		783	863
[UO₂(CO₃)(H₂O)(R′Ac)₂]²⁻	1.805			2.393	2.354	2.638	810	890
[UO₂(R′Ac)₃]⁻	1.785			2.515			848	932
[UO₂(CO₃)(H₂O)(R′AO)(R′Ac)]²⁻	1.810		2.406	2.362	2.324	2.880	801	882
UO₂(H₂O)₂(R′AO)(R′Ac)	1.787	2.394	2.287	2.529		2.589	846	932
[UO₂(R′AO)₂(R′Ac)]⁻	1.799	2.428	2.374	2.556			822	903
[UO₂(R′AO)(R′Ac)₂]⁻	1.793	2.408	2.358	2.532			833	916
[UO₂(CO₃)(H₂O)(R′₂HA)]⁻	1.802	2.710	2.571		2.332	2.737	811	897
[UO₂(H₂O)₃(R′₂HA)]⁺	1.773	2.576	2.410			2.628	871	958
UO₂(R′₂HA)₂	1.786	2.670	2.491				841	928
UO₂(H₂O)(R′₂HA)(R′Ac)	1.782	2.621	2.468	2.498		2.594	852	938

radii using the "SCRF=COSMO" keyword in the Gaussian 09 program package. The reliability of our theoretical methods for prediction of structure parameters was also evaluated by optimizing the geometrical structures of two model uranyl complexes in the gas phase and aqueous solution at the B3LYP/6-311G(d, p)/RECP level of theory (see Figure S1 in Supporting Information). According to our calculations, the predicted bond distances in the gas phase are found to be in accordance with those in aqueous solution. Additionally, for the small ionic molecule H₃O⁺, experimental data of solvation free energy (−110.2 kcal/mol)[47,48] were used for calculations. For other species, the Gibbs free energy in aqueous solution was obtained by adding the solvation free energy to the gas-phase Gibbs free energy. Previous studies[49,50] confirmed that single-point calculations based on the gas-phase geometries are sufficient for solvation energy prediction because reoptimizing structures in solvent shows little influence on the energetics.

3. RESULTS AND DISCUSSION

3.1. Uranyl Complexes with Acetamidoxime (R′AO⁻, R′=CH₃), Acetate (R′Ac⁻), Dimethyl Glutarimidedioximate (R′₂HA⁻), and Carbonate (CO₃²⁻) Groups. *3.1.1. Geometrical Structures.* A series of uranyl complexes with acetamidoxime (R′AO⁻, R′=CH₃), acetate (R′Ac⁻), dimethyl glutarimidedioxime (R′₂HA⁻), and carbonate (CO₃²⁻) were optimized at the B3LYP/6-311G(d, p)/RECP level of theory. Various structures with different ligand binding motifs were evaluated to obtain the relatively stable geometrical structures. Initial calculations included three possible binding motifs for acetamidoxime (Figure 1a−c) and two possible binding modes (bidentate and monodentate) for acetate. Besides, the representative tridentate and bidentate binding motifs were taken into account for glutarimidedioxime and carbonate, respectively. All the optimized structures are shown in Supporting Information, Figure S2, and the relatively stable isomers are depicted in Figure 2. For the unsaturated species, water molecules were added to saturate the equatorial coordination, which results in five- or six-membered chelate rings in the equatorial plane of uranyl ion (Figure 2).

As shown in Figure 2, for most of these relatively stable complexes, R′AO and R′Ac are usually coordinated as bidentate ligands. However, [UO₂(CO₃)₂(R′AO)]³⁻ and [UO₂(CO₃)(H₂O)(R′AO)₂]²⁻ complexes with monodentate R′AO are more stable than those with bidentate R′AO, which may be attributed to the intramolecular hydrogen bonding between

hydrogen atoms in the amido group of R′AO and oxygen atoms of carbonate ion. In the case of [UO₂(CO₃)₂(R′Ac)]³⁻ and [UO₂(CO₃)(H₂O)(R′Ac)₂]²⁻, the monodentate binding modes are also preferable for R′Ac. We note that in these two species, except for the hydrogen bonding between R′AO and carbonate ion, the methyl hydrogen atoms and uranyl oxygen atoms also form intramolecular hydrogen bonding. Therefore, the formation of hydrogen bonds enhance the stability of these species.

As listed in Table 1, the uranyltricarbonate complex [UO₂(CO₃)₃]⁴⁻ exhibits the longest average bond distances between uranium and axial oxygen atoms among all of these complexes, suggesting the weaker U=O(axial) bonds in [UO₂(CO₃)₃]⁴⁻ compared to other species. For [UO₂(CO₃)₂(R′AO)]³⁻, [UO₂(CO₃)(H₂O)(R′AO)₂]²⁻ and [UO₂(R′AO)₃]⁻, the average U=O(axial) bond distances are longer than those in complexes with R′Ac⁻ groups. This indicates that the U=O(axial) bonds are weakened to a larger extent by R′AO⁻ than by R′Ac⁻. Alternatively, the calculated U−O(R′AO⁻) bond distances are shorter than the U−O(R′Ac⁻) distances. As for the uranyl complexes with both R′AO⁻ and R′Ac⁻ ligands (R′AO⁻/R′Ac⁻), the U=O(axial) distances in [UO₂(CO₃)(H₂O)(R′AO)(R′Ac)]²⁻ are longer than those in other species, implying that the U=O(axial) bonds are the most weakest in these species. However, UO₂(H₂O)₂(R′AO)(R′Ac) shows the shortest U=O(axial) distances, which may be due to the relatively weaker coordination ability of water molecules to uralyl cation. For complexing species with R′₂HA⁻, the U=O(axial) distances decrease in the order of [UO₂(CO₃)(H₂O)(R′₂HA)]⁻ > UO₂(R′₂HA)₂ > UO₂(H₂O)(R′₂HA)(R′Ac) > [UO₂(H₂O)₃(R′₂HA)]⁺. The symmetrical and antisymmetrical stretching frequencies (v_s and v_{as}) of U=O(axial) show the same results with the U=O(axial) distances, which also reflect the coordination ability of ligands. Moreover, for each species with R′AO⁻ coordinated in η^2 binding mode and the tridentate R′₂HA⁻ ligands, the U−N(R′AO⁻/R′₂HA⁻) bond distances are predicted to be much longer compared to the U−O(R′AO⁻/R′₂HA⁻) bond distances, suggesting that the oxime oxygen atom has stronger binding strength than the oxime nitrogen atom.

3.1.2. NBO Analysis. The bonding nature of these uranyl complexes including bond orders and atomic charges have been investigated by the natural bond orbital (NBO) analysis[40−43] at the B3LYP/6-311G(d, p)/RECP level of theory (Table 2). For

Table 2. Wiberg Bond Indices (WBIs) of U−N and U−O Bonds and Natural Charges on U Atoms and Transfer of Charges from Ligands to Metal Atoms by the B3LYP Method

species	U−N (R'AO$^-$/R'$_2$HA$^-$)	U−O (R'AO$^-$/R'$_2$HA$^-$)	U−O (R'Ac$^-$)	U−O (CO$_3^{2-}$)	U−O (H$_2$O)	Q(U)	ΔQ (R'AO$^-$/R'$_2$HA$^-$)	ΔQ (R'Ac$^-$)	ΔQ (CO$_3^{2-}$)	ΔQ (H$_2$O)
$[UO_2(CO_3)_2(R'AO)]^{3-}$		0.698		0.570		1.417	0.388		0.715	
$[UO_2(CO_3)(H_2O)(R'AO)_2]^{2-}$		0.768		0.599	0.208	1.379	0.468		0.776	0.082
$[UO_2(R'AO)_3]^-$	0.436	0.603				1.210	0.620			
$[UO_2(CO_3)_2(R'Ac)]^{3-}$			0.489	0.597		1.484		0.278	0.738	
$[UO_2(CO_3)(H_2O)(R'Ac)_2]^{2-}$			0.573	0.651	0.333	1.470		0.366	0.821	0.319
$[UO_2(R'Ac)_3]^-$			0.443			1.486		0.534		
$[UO_2(CO_3)(H_2O)(R'AO)(R'Ac)]^{2-}$	0.520	0.629	0.585	0.695	0.229	1.442	0.419	0.368	0.861	0.085
$UO_2(H_2O)_2(R'AO)(R'Ac)$	0.468	0.766	0.424		0.346	1.362	0.781	0.522		0.192
$[UO_2(R'AO)_2(R'Ac)]^-$	0.488	0.625	0.396			1.284	0.656	0.480		
$[UO_2(R'AO)(R'Ac)_2]^-$		0.658	0.419			1.380	0.690	0.506		
$[UO_2(CO_3)(H_2O)(R'_2HA)]^-$	0.317	0.449		0.698	0.297	1.384	0.712		0.897	0.144
$[UO_2(H_2O)_3(R'_2HA)]^+$	0.407	0.580			0.343	1.502	0.546			0.189
$UO_2(R'_2HA)_2$	0.356	0.527				1.393	0.837			
$UO_2(H_2O)(R'_2HA)(R'Ac)$	0.373	0.536	0.463		0.357	1.434	0.858	0.564		0.196

$[UO_2(CO_3)_2(R'AO)]^{3-}$, $[UO_2(CO_3)(H_2O)(R'AO)_2]^{2-}$, and $[UO_2(R'AO)_3]^-$, the Wiberg bond indices (WBIs) of the U−O(R'AO$^-$) bonds are much larger than those of the corresponding U−O(R'Ac$^-$) bonds in $[UO_2(CO_3)_2(R'Ac)]^{3-}$, $[UO_2(CO_3)(H_2O)(R'Ac)_2]^{2-}$, and $[UO_2(R'Ac)_3]^-$. Similar trends can be observed for the species with R'AO$^-$/R'Ac$^-$ ligands. These results suggest that the U−O bonds in complexes of acetamidoxime groups have more covalent character than those in acetate complexes. Additionally, compared with the U−N(R'AO$^-$) bonds in complexes with R'AO$^-$ coordinated as η^2 binding mode, the U−O(R'AO$^-$) bonds show larger WBIs, implying the stronger electron transfer ability of the oxime oxygen atom. As for complexes with R'$_2$HA$^-$ group, the WBIs of the U−O(R'$_2$HA$^-$) bonds are also larger than those of the U−N(R'$_2$HA$^-$) bonds, which suggests that the bonds between the uranium and oxime oxygen atom exhibit higher degree of covalent character.

On the basis of the natural population analysis (NPA), the natural charges on uranium atoms for all of these complexes are much lower than those for the free uranyl cation (2.736), indicating significant electron-donation from the ligands to uranium. As for $[UO_2(CO_3)_2(R'AO)]^{3-}$, $[UO_2(CO_3)(H_2O)(R'AO)_2]^{2-}$, and $[UO_2(R'AO)_3]^-$, the net charges on uranium atoms are lower than those for the corresponding R'Ac$^-$ analogues. This confirms that the R'AO$^-$ ligands exhibit larger electron-donating ability to uranium. Compared to $[UO_2(CO_3)(H_2O)(R'Ac)_2]^{2-}$, the uranium atom in $[UO_2(CO_3)(H_2O)(R'AO)(R'Ac)]^{2-}$ shows lower natural charges, which is even higher than that for $[UO_2(CO_3)(H_2O)(R'AO)_2]^{2-}$. Similarly, as for $[UO_2(R'AO)(R'Ac)_2]^-$, the uranium atom remains higher net charges than $[UO_2(R'AO)_2(R'Ac)]^-$. Alternatively, for all of these species, the ligand-to-metal charge transfer was higher in the case of R'AO$^-$ compared to R'Ac$^-$. These results give another evidence of the stronger electron-donating ability of the R'AO$^-$ ligands. Nevertheless, according to the ligand-to-metal charge transfer in $UO_2(H_2O)(R'_2HA)(R'Ac)$ and $UO_2(H_2O)_2(R'AO)(R'Ac)$, we can deduce that R'$_2$HA$^-$ has stronger electron-donating ability than R'AO$^-$, which is probably due to the tridentate coordination of the R'$_2$HA$^-$ ligands. Moreover, the carbonate groups exhibit larger charge transfers than other groups. This may be caused by the divalent ligands of the carbonate groups, which are more obviously affected by the electrostatic attraction than the monovalent ligands of R'AO$^-$, R'Ac$^-$, and R'$_2$HA$^-$.

3.1.3. Molecular Orbital (MO) Analysis. To further probe the nature of metal−ligand bonding in the uranyl complexes, we calculated the MOs of six model complexes at the B3LYP/6-311G(d, p)/RECP level of theory, and some relevant MOs are illustrated in Figure 4. The MO plots give a pictorial description of the U−O and U−N σ-bonding, which mainly originate from the interaction of U 6d, 5f orbitals and O, N 2p orbitals. Besides, in $[UO_2(R'AO)_3]^-$, $[UO_2(R'AO)_2(R'Ac)]^-$, and $[UO_2(R'AO)(R'Ac)_2]^-$, the U−O(R'AO$^-$) π-bonding resides in the higher-energy MOs (Figure S3 in Supporting Information), which results from the interactions between U 5f orbitals and O 2p orbitals.

In addition to these delocalized MOs, some localized orbitals are obtained from NBO analysis (Supporting Information, Figures S4−S10), which can provide more chemically relevant information on the metal−ligand bonding. For $[UO_2(R'AO)_3]^-$, U−O and U−N σ-bonds contain 12% uranium and 88% oxygen or nitrogen character, while U−O π-bonds contain 4% uranium and 96% oxygen character. For U−O π-bonds, the uranium

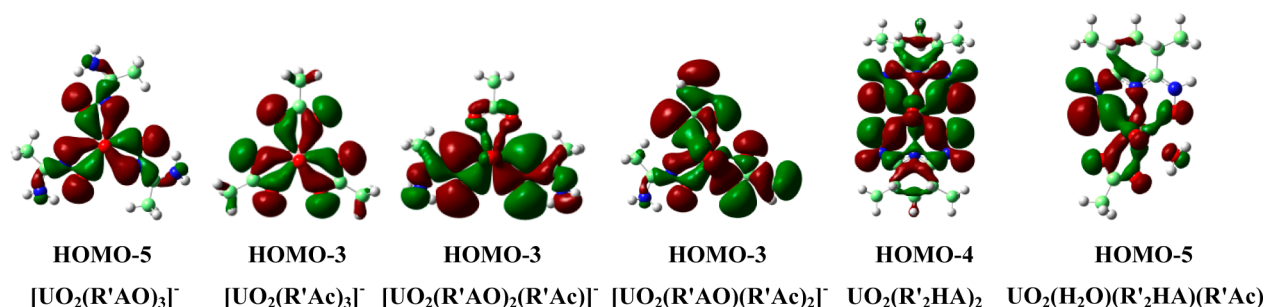|					
HOMO-5	HOMO-3	HOMO-3	HOMO-3	HOMO-4	HOMO-5
$[UO_2(R'AO)_3]^-$	$[UO_2(R'Ac)_3]^-$	$[UO_2(R'AO)_2(R'Ac)]^-$	$[UO_2(R'AO)(R'Ac)_2]^-$	$UO_2(R'_2HA)_2$	$UO_2(H_2O)(R'_2HA)(R'Ac)$

Figure 4. Main molecular orbitals of the uranyl complexes contributing to the metal−ligand bonding.

Table 3. Metal-Ligand Binding Energies (kcal/mol) for Uranyl Complexes with $R'AO^-$, $R'Ac^-$, R'_2HA^-, and CO_3^{2-} in the Gas Phase and Aqueous Solution

reactions	ΔG_g	ΔG_{sol}
$[UO_2(H_2O)_5]^{2+} + 3CO_3^{2-} \rightarrow [UO_2(CO_3)_3]^{4-} + 5H_2O$	−457.9	−152.9
$[UO_2(H_2O)_5]^{2+} + 2CO_3^{2-} + R'AO^- \rightarrow [UO_2(CO_3)_2(R'AO)]^{3-} + 5H_2O$	−531.4	−144.1
$[UO_2(H_2O)_5]^{2+} + CO_3^{2-} + 2R'AO^- \rightarrow [UO_2(CO_3)(H_2O)(R'AO)_2]^{2-} + 4H_2O$	−656.7	−67.8
$[UO_2(H_2O)_5]^{2+} + 3R'AO^- \rightarrow [UO_2(R'AO)_3]^- + 5H_2O$	−420.6	−122.7
$[UO_2(H_2O)_5]^{2+} + 2CO_3^{2-} + R'Ac^- \rightarrow [UO_2(CO_3)_2(R'Ac)]^{3-} + 5H_2O$	−525.5	−128.4
$[UO_2(H_2O)_5]^{2+} + CO_3^{2-} + 2R'Ac^- \rightarrow [UO_2(CO_3)(H_2O)(R'Ac)_2]^{2-} + 4H_2O$	−498.2	−96.8
$[UO_2(H_2O)_5]^{2+} + 3R'Ac^- \rightarrow [UO_2(R'Ac)_3]^- + 5H_2O$	−383.5	−76.0
$[UO_2(H_2O)_5]^{2+} + CO_3^{2-} + R'AO^- + R'Ac^- \rightarrow [UO_2(CO_3)(H_2O)(R'AO)(R'Ac)]^{2-} + 5H_2O$	−506.5	−104.5
$[UO_2(H_2O)_5]^{2+} + R'AO^- + R'Ac^- \rightarrow UO_2(H_2O)_2(R'AO)(R'Ac) + 3H_2O$	−363.5	−73.0
$[UO_2(H_2O)_5]^{2+} + 2R'AO^- + R'Ac^- \rightarrow [UO_2(R'AO)_2(R'Ac)]^- + 5H_2O$	−410.8	−108.8
$[UO_2(H_2O)_5]^{2+} + R'AO^- + 2R'Ac^- \rightarrow [UO_2(R'AO)(R'Ac)_2]^- + 5H_2O$	−398.4	−93.8
$[UO_2(H_2O)_5]^{2+} + CO_3^{2-} + R'_2HA^- \rightarrow [UO_2(CO_3)(H_2O)(R'_2HA)]^- + 4H_2O$	−509.7	−102.1
$[UO_2(H_2O)_5]^{2+} + R'_2HA^- \rightarrow [UO_2(H_2O)_3(R'_2HA)]^+ + 2H_2O$	−237.4	−49.8
$[UO_2(H_2O)_5]^{2+} + 2R'_2HA^- \rightarrow UO_2(R'_2HA)_2 + 5H_2O$	−355.7	−89.4
$[UO_2(H_2O)_5]^{2+} + R'_2HA^- + R'Ac^- \rightarrow UO_2(H_2O)(R'_2HA)(R'Ac) + 4H_2O$	−344.2	−73.6

Table 4. Changes of the Gibbs Free Energy (kcal/mol) for the Reactions of Uranyl Complexes with $R'AO^-$, $R'Ac^-$, R'_2HA^-, and CO_3^{2-} in the Gas Phase and Aqueous Solution

reactions	ΔG_g	ΔG_{sol}
$[UO_2(CO_3)_3]^{4-} + R'HAO \rightarrow [UO_2(CO_3)_2(R'AO)]^{3-} + HCO_3^-$	−212.6	2.5
$[UO_2(CO_3)_2(R'AO)]^{3-} + R'HAO + H_2O \rightarrow [UO_2(CO_3)(H_2O)(R'AO)_2]^{2-} + HCO_3^-$	−123.9	14.9
$[UO_2(CO_3)(H_2O)(R'AO)_2]^{2-} + R'HAO \rightarrow [UO_2(R'AO)_3]^- + HCO_3^- + H_2O$	−43.6	−6.1
$[UO_2(CO_3)_3]^{4-} + R'HAc \rightarrow [UO_2(CO_3)_2(R'Ac)]^{3-} + HCO_3^-$	−227.2	−3.9
$[UO_2(CO_3)_2(R'Ac)]^{3-} + R'HAc + H_2O \rightarrow [UO_2(CO_3)(H_2O)(R'Ac)_2]^{2-} + HCO_3^-$	−132.3	3.3
$[UO_2(CO_3)(H_2O)(R'Ac)_2]^{2-} + R'HAc \rightarrow [UO_2(R'Ac)_3]^- + HCO_3^- + H_2O$	−44.9	−7.6
$[UO_2(CO_3)_3]^{4-} + R'HAO + R'HAc + H_2O \rightarrow [UO_2(CO_3)(H_2O)(R'AO)(R'Ac)]^{2-} + 2HCO_3^-$	−347.4	13.7
$[UO_2(CO_3)_3]^{4-} + R'HAO + R'HAc + 2H_2O \rightarrow UO_2(H_2O)_2(R'AO)(R'Ac) + 2HCO_3^- + CO_3^{2-}$	−204.3	45.2
$[UO_2(CO_3)_3]^{4-} + 2R'HAO + R'HAc \rightarrow [UO_2(R'AO)_2(R'Ac)]^- + 3HCO_3^-$	−390.8	3.1
$[UO_2(CO_3)_3]^{4-} + R'HAO + 2 R'HAc \rightarrow [UO_2(R'AO)(R'Ac)_2]^- + 3HCO_3^-$	−398.9	−3.9
$[UO_2(CO_3)_3]^{4-} + R'_2H_2A + H_2O \rightarrow [UO_2(CO_3)(H_2O)(R'_2HA)]^- + HCO_3^- + CO_3^{2-}$	−202.7	37.9
$[UO_2(CO_3)_3]^{4-} + R'_2H_2A + 3H_2O \rightarrow [UO_2(H_2O)_3(R'_2HA)]^+ + HCO_3^- + 2CO_3^{2-}$	69.7	90.1
$[UO_2(CO_3)_3]^{4-} + 2R'_2H_2A \rightarrow UO_2(R'_2HA)_2 + 2HCO_3^- + CO_3^{2-}$	−179.5	37.7
$[UO_2(CO_3)_3]^{4-} + R'_2H_2A + R'HAc + H_2O \rightarrow UO_2(H_2O)(R'_2HA)(R'Ac) + 2HCO_3^- + CO_3^{2-}$	−196.7	38.0

component is composed of about 63% 5f orbital character, which is much higher than that for U−O (24%) and U−N (20%) σ-bonds. As for $[UO_2(R'Ac)_3]^-$, only U−O σ-bonds have been observed, which are composed of 10% uranium and 90% oxygen character and contain 21% 5f orbital character and 76% 2p orbital character for uranium and oxygen, respectively. For the complex of $UO_2(R'_2HA)_2$, the U−O σ-bonds contain 11% uranium and 89% oxygen character, and the uranium component is composed of 23% 5f orbital character. Similar results can be found in the U−N σ-bonds. In the case of complexing species with mixed groups, $[UO_2(R'AO)_2(R'Ac)]^-$, $[UO_2(R'AO)(R'Ac)_2]^-$, and $UO_2(H_2O)(R'_2HA)(R'Ac)$, the U−O(R'AO) σ- and π-bonds

are also observed, and the uranium components of the 5f orbital characters are slightly higher than those in $[UO_2(R'AO)_3]^-$, $[UO_2(R'Ac)_3]^-$, and $UO_2(R'_2HA)_2$, for example, the uranium component of the U−O π-bonds in $[UO_2(R'AO)(R'Ac)_2]^-$ is composed of about 78% 5f orbital character. These results indicate that introduction of $R'Ac^-$ groups can increase the uranium 5f orbital characters of the metal−ligand bonding.

3.1.4. Thermodynamic Stability. To estimate the thermodynamic stability of these uranyl complexes, the metal−ligand binding energies of these complexes with uranyl pentahydrate $[UO_2(H_2O)_5]^{2+}$ as reactants were calculated at the B3LYP/6-311G(d, p)/RECP level of theory in the gas phase and aqueous

solution. As listed in Table 3, the gas phase and hydration binding energies for $[UO_2(CO_3)_3]^{4-}$ are −457.9 and −152.9 kcal/mol, respectively. For uranyl species with R′AO⁻, R′Ac⁻, R′₂HA⁻, the gas phase binding energies are between −237.4 and −656.7 kcal/mol, which are more negative than the hydration binding energies for the corresponding species (from −49.8 to −144.1 kcal/mol). This indicates that these species are all stable in the gas phase, whereas their stabilities decrease significantly in aqueous solution. This is mainly attributed to the very strong electrostatic interactions between the metal and ligands in the gas phase, while in aqueous solution these interactions are partially counteracted by solvent effects. As shown in Table 4, $[UO_2(CO_3)_2(R′AO)]^{3-}$ and $[UO_2(R′AO)_3]^{-}$ complexes possess more negative binding energies than the corresponding R′Ac⁻ analogues, which indicates that these R′AO⁻ complexes are more stable than their R′Ac⁻ analogues. As for the complexes with R′AO⁻/R′Ac⁻ ligands, the absolute values of the negative binding energies are in the order of $[UO_2(R′AO)_2(R′Ac)]^{-}$ > $[UO_2(CO_3)(H_2O)(R′AO)(R′Ac)]^{2-}$ > $[UO_2(R′AO)(R′Ac)_2]^{-}$ > $UO_2(H_2O)_2(R′AO)(R′Ac)$, suggesting that the stabilities of these species follow the same order. Compared with $[UO_2(R′AO)_3]^{-}$, $[UO_2(R′AO)_2(R′Ac)]^{-}$ have lower binding energy, while the binding energy of $[UO_2(R′AO)(R′Ac)_2]^{-}$ is higher than that of $[UO_2(R′Ac)_3]^{-}$, which indicates that the R′AO⁻ ligands have a stronger ability to stabilize the uranyl cations. For the complexes with R′₂HA⁻ ligands, $[UO_2(CO_3)(H_2O)(R′_2HA)]^{-}$ have the most negative gas phase and hydration binding energy, while the corresponding species without carbonate ligand $[UO_2(H_2O)_3(R′_2HA)]^{+}$ exhibit the lowest binding energy. In addition, $UO_2(H_2O)(R′_2HA)(R′Ac)$ and $UO_2(H_2O)_2(R′AO)(R′Ac)$ show comparable binding energy.

3.1.5. Possible Interaction Mechanism. To explore the interaction mechanisms of uranium extraction, we considered a series of displacement reactions as the possible adsorption reactions by the B3LYP method (Table 4). For all of these reactions except $[UO_2(CO_3)_3]^{4-} + R′_2H_2A + 3H_2O \rightarrow [UO_2(H_2O)_3(R′_2HA)]^{+} + HCO_3^{-} + 2CO_3^{2-}$, the changes of Gibbs free energy are found to be negative in the gas phase (298.15 K, 0.1 MPa), indicating that these reactions can be spontaneous in the gas phase. The exception of the reaction involving $[UO_2(H_2O)_3(R′_2HA)]^{+}$ may be attributed to the significantly lower metal−ligand binding energy of $[UO_2(H_2O)_3(R′_2HA)]^{+}$ than $[UO_2(CO_3)_3]^{4-}$. However, the changes of Gibbs free energy for these reactions dramatically decrease when solvent effects are taken into account in the calculations, and most of the reactions are endothermic. This indicates that many of the displacement reactions considered here may not occur in aqueous solutions. Nevertheless, some useful results can be obtained from analyzing tendencies of these reactions.

For the displacement reactions with the carbonate groups displaced by the acetamidoxime groups, the reaction energies are found to be lower than the corresponding reactions of the uranyl complexes with acetate groups. This result seems to be contrary to the conclusion based on the binding energies for these species, that is, the species with R′AO⁻ are more stable compared to those with R′Ac⁻. Previous studies[20−22] indicate that the hydrogen ions from the hydrophilic groups can promote $[UO_2(CO_3)_3]^{4-}$ dissociation to UO_2^{2+}. We thus calculated the reaction energies of $R′HAO + H_2O \rightarrow H_3O^{+} + R′AO^{-}$ and $R′HAc + H_2O \rightarrow H_3O^{+} + R′Ac^{-}$ and found that R′HAc release hydrogen ions much more easily than the R′HAO release these

ions. Therefore, R′HAc makes it more available for the displacement reactions compared with R′HAO. As for adsorption reactions of uranyl by R′AO⁻/R′Ac⁻ ligands, the gas phase reaction energies are more negative than those for reactions with R′AO⁻ or R′Ac⁻. However, these reactions have very low changes of Gibbs free energy in aqueous solution. Even so, compared to the reactions with R′AO⁻, the reactions with R′AO⁻/R′Ac⁻ ligands exhibit lower reaction energies, indicating that the presence of R′Ac⁻ ligands can increase the U(VI) adsorption efficiency. In the case of the displacement reactions with R′₂HA⁻ in aqueous solution, all the reaction energies are found be positive, indicating that they are not spontaneous reactions at the temperature of 298.15 K. Furthermore, we also explored the temperature effects on the thermodynamics for reactions of R′AO⁻ and R′₂HA⁻ with complexes optimized in aqueous solution (Supporting Information, Table S2), and found that most of these reactions are still highly endothermic at higher temperature and seem to be difficult to occur in aqueous solution. However, for reactions of $[UO_2(CO_3)_2(R′AO)]^{3-}$ and $[UO_2(R′AO)_3]^{-}$, the calculated ΔG_{sol} values become more negative with the rise of temperature, indicating that these reactions could be promoted at higher temperature. The marine experiments in Japan[24] confirmed that the U(VI) extraction efficiency can be improved at higher temperatures, and the complexation of uranyl with amidoxime is the rate-determining step with activation energy of about 20 kcal/mol for uranium extraction.

To elucidate the reaction kinetics of the uranyl tricarbonate complex $[UO_2(CO_3)_3]^{4-}$ with the amidoxime group, stationary points on the reaction pathway have been explored in aqueous solution with the relatively accessible reaction $[UO_2(CO_3)_3]^{4-} + R′HAO \rightarrow [UO_2(CO_3)_2(R′AO)]^{3-} + HCO_3^{-}$ as the model reaction. Our hypothesis is that this displacement reaction consists of the following two steps: (i) the formation of the monodentate carbonate group combined with complexation of $[UO_2(CO_3)_3]^{4-}$ and R′HAO via an intermolecular hydrogen bond between the oxime and the carbonate group; (ii) proton migration from R′HAO to carbonate group accompanied by coordination of amidoxime to the uranium center. To make the reaction kinetic simulation model closer to the actual experimental situation, all the complex species referring to this reaction were fully optimized in aqueous solution at the B3LYP/6-311G(d, p)/RECP level of theory, and the obtained potential energy profile is presented in Figure 5. We also tried to analyze the gas phase reaction kinetics of this complexing process, and found that the intermediates and transition states obtained in aqueous solution turn out to be unstable in the gas phase. This is probably because the solvent effect affects the reaction kinetics and enhances the stability of the transition states and intermediates. From Figure 5, it can be seen that the concerted hydrogen migration, that is, the coordination of the uranyl cation to the amidoxime group and the dissociation of the carbonate group, is the rate-determining step with overall free energy barrier of 20.1 kcal/mol, which is close to the experimental result.[24] Considering that other endothermic displacement reactions show higher changes of Gibbs free energy compared to $[UO_2(CO_3)_3]^{4-} + R′HAO \rightarrow [UO_2(CO_3)_2(R′AO)]^{3-} + HCO_3^{-}$ (Table 4), those reactions appear to be more difficult to proceed in aqueous solution. Note that the ΔG_{sol} values for this reaction with all species optimized in aqueous solution are nearly 3.0 kcal/mol lower than those corresponding results derived from previous approach, which combines gas-phase optimization and solvation energy calculation mentioned above. That is to say,

9471

dx.doi.org/10.1021/ic500202g | *Inorg. Chem.* 2014, 53, 9466−9476
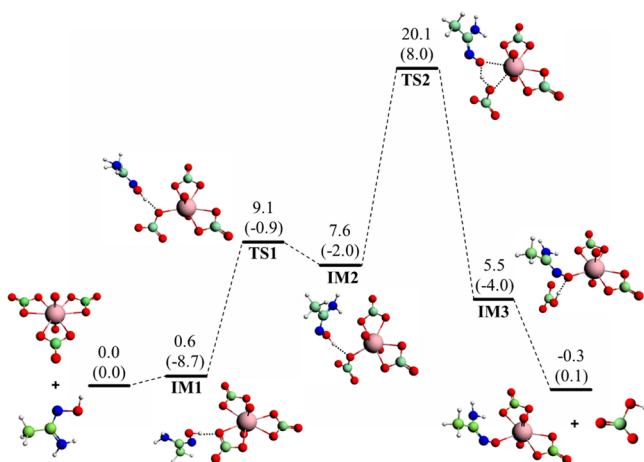
Figure 5. Energy profiles calculated for the displacement reaction $[UO_2(CO_3)_3]^{4-}$ + R'HAO → $[UO_2(CO_3)_2(R'AO)]^{3-}$ + HCO_3^- with species fully optimized in aqueous solution. Values refer to relative Gibbs free energies, and relative electronic energies (in parentheses) are given in kcal/mol. IM and TS denote the intermediate and transition state, respectively.

geometry optimization in the aqueous solution environment would lead to small decrease of Gibbs free energy changes compared to the previous approach, and this difference seems to be important for reactions with small ΔG_{sol} (0–3 kcal/mol) values.

3.2. Uranyl Complexes with R''AO⁻, R''Ac⁻, and R''HA⁻ on a Single Alkyl Chain (R''=C₁₃H₂₆). Previous studies[17−24] reported that amidoxime-based polymer adsorbents can be prepared by radiation-induced grafting technique, in which nitriles or mixtures of nitrile and acid are grafted onto polymers, and then convert cyano groups into amidoxime groups by reacting the grafted polymers with hydroxylamine. To understand the interactions between amidoxime-based polymers and uranyl ions, simple analogues with AO⁻, Ac⁻, and HA⁻ on alkyl chain (R''=C₁₃H₂₆) were selected as model ligand chains to investigate the coordination modes and stabilities of the uranyl complexes.

Since the long alkyl chain (R''=C₁₃H₂₆) has a lot of strain, and its structure can be reorganized when complexing with uranyl cation, several initial structures with different curvatures were optimized in aqueous solution. Figure 6 shows the relatively stable geometrical structures of the ligand chains. It can be seen that in (R''HAO)₂, (R''HAc)₂, and R''HAO/HAc, the alkyl chains are nearly linear, and the ligands usually adopt the *trans* structure, which can minimize the repulsive forces of the ligands on the chain.

All the optimized structures of uranyl complexes with R''AO⁻, R''Ac⁻, R''HA⁻ groups on a single alkyl chain (R''=C₁₃H₂₆) are shown in Supporting Information, Figure S11, and the relatively stable structures are given in Figure 7. Besides, in the unsaturated

species, water molecules are added in the uranyl equatorial plane (Figure 7). As expected, in these species, the ligand chains reorganize their structures to coordinate with uranyl cations. It can be seen that the R''AO⁻ groups mainly coordinate in η^2-binding modes to the uranyl cations, while R''Ac⁻ and R''HA⁻ groups prefer to coordinate as monodentate and tridentate ligands, respectively. The U−N(R''AO⁻) bond distances are longer than the U−O(R''AO⁻) bonds (Supporting Information, Table S3). Alternatively, the WBIs of the U−O(R''AO⁻) bonds are found to be larger than U−N(R''AO⁻) (Supporting Information, Table S4). Similar trends can be observed in the R''HA⁻ groups. These confirm that for R''AO⁻ and R''HA⁻ groups, the oxygen atoms have higher complexing ability to the uranyl cations. In addition, the natural charges on the U atoms in these species are much smaller than those of free uranyl ions (2.736), indicating significant electron donation from ligands to uranium.

A series of reactions with $[UO_2(CO_3)_3]^{4-}$ as reactant have been calculated in the gas phase and aqueous solution to further explore the adsorption process of uranium (Table 5). Except for the reaction with $[UO_2(R''HA)(H_2O)]^+$, for all these reactions the changes of Gibbs free energy are all negative in the gas phase. In contrast, most of them change to large positive values in aqueous solution, indicating that these reactions are highly endothermic, and the single alkyl ligand chain may not react with $[UO_2(CO_3)_3]^{4-}$ based on our calculated results. Actually, some reactions with small positive Gibbs free energy changes deriving from the gas-phase geometry optimization approach may also occur, given that geometry optimization in aqueous solution can result in the decrease of the Gibbs free energy of reaction by about 3.0 kcal/mol. Comparing the ΔG values in aqueous solution (ΔG_{sol}), $[UO_2(CO_3)(R''AO)_2]^{2-}$, $UO_2(CO_3)(R''Ac)_2(H_2O)]^{2-}$, $[UO_2(CO_3)(R''AO/Ac)]^{2-}$, and $[UO_2(CO_3)(R''HA)]^-$ are found to be more favorable energetically than the corresponding complexes without carbonate groups, suggesting that the carbonate groups prevent the further adsorption of uranium. Besides, the formation of $[UO_2(CO_3)(R''AO)(R''Ac)]^{2-}$ are found to be more easily compared to $[UO_2(CO_3)(R''AO)_2]^{2-}$. Thus, as reported in literature,[20−22] absorbents with both AO⁻ and Ac⁻ can increase the adsorption ability to the uranyl ions.

3.3. Uranyl Complexes with R''AO⁻, R''Ac⁻, and R''HA⁻ on Double Alkyl Chains (R''=C₁₃H₂₆). For the charged and neutral uranyl complexes with R''AO⁻, R''Ac⁻, and R''HA⁻ groups on double alkyl chains (R''=C₁₃H₂₆), all the optimized structures with ligands in different binding motifs are depicted in Supporting Information, Figure S12. In the relatively stable structures (Figures 8 and 9), the R''AO⁻ groups can coordinate as η^2 mode and monodentate ligands, while the R''Ac⁻ and R''HA⁻ groups are monodentate and tridentate ligands to the uranyl cations, respectively. As for complexing species with R''AO⁻ as η^2 ligands and those with R''HA⁻ as tridentate ligands, the U−O(R''AO⁻/R''HA⁻) bonds have shorter bond distances
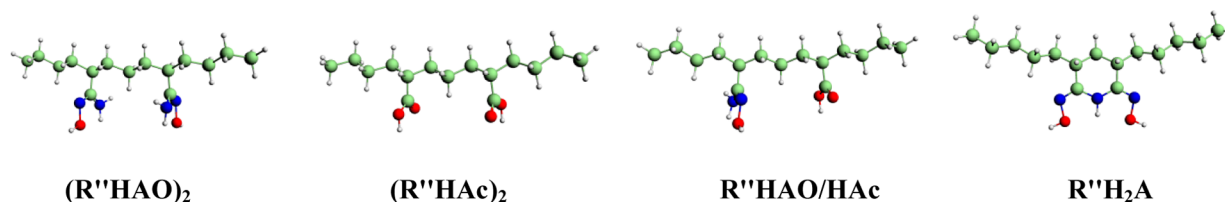
Figure 6. Optimized structures for ligand chains of (R''HAO)₂, (R''HAc)₂, R''HAO/HAc, and R''H₂A (R''=C₁₃H₂₆).
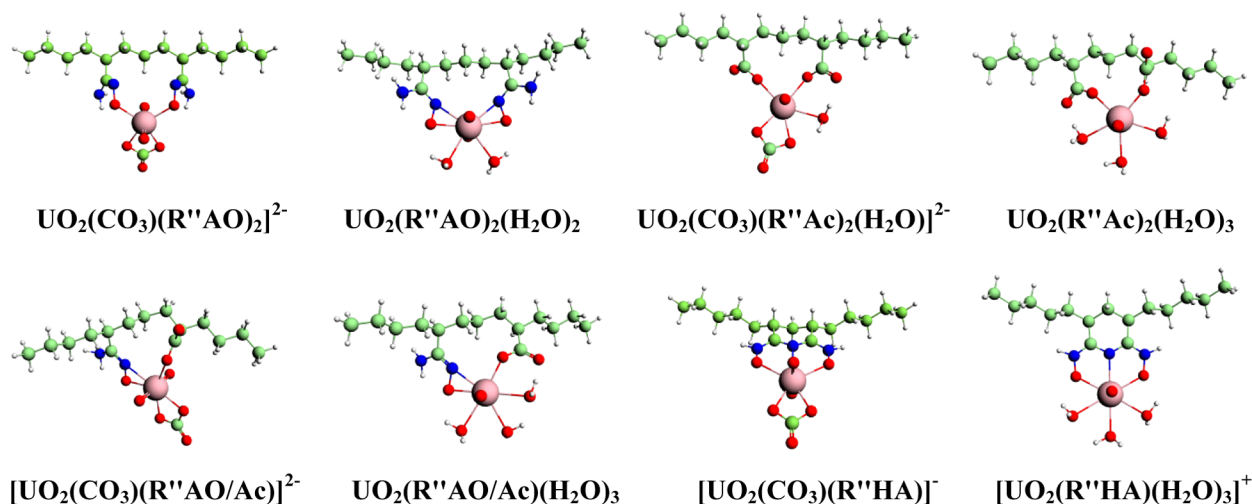
Figure 7. Optimized structures of uranyl complexes with R″AO⁻, R″Ac⁻, and R″HA⁻ on a single alkyl chain (R″=$C_{13}H_{26}$).

Table 5. Changes of the Gibbs Free Energy (kcal/mol) for the Reactions of Uranyl Complexes with R″AO⁻, R″Ac⁻, and R″HA⁻ on a Single Alkyl Chain (R″=$C_{13}H_{26}$) in the Gas Phase and Aqueous Solution

reactions	ΔG_g	ΔG_{sol}
$[UO_2(CO_3)_3]^{4-}$ + (R″HAO)$_2$ → $[UO_2(CO_3)(R″AO)_2]^{2-}$ + 2HCO$_3^-$	−336.6	15.1
$[UO_2(CO_3)_3]^{4-}$ + (R″HAO)$_2$ + 2H$_2$O → UO$_2$(R″AO)$_2$(H$_2$O)$_2$ + 2HCO$_3^-$ + CO$_3^{2-}$	−193.3	52.3
$[UO_2(CO_3)_3]^{4-}$ + (R″HAc)$_2$ + H$_2$O → $[UO_2(CO_3)(R″Ac)_2(H_2O)]^{2-}$ + 2HCO$_3^-$	−366.3	−2.0
$[UO_2(CO_3)_3]^{4-}$ + (R″HAc)$_2$ + 3H$_2$O → UO$_2$(R″Ac)$_2$(H$_2$O)$_3$ + 2HCO$_3^-$ + CO$_3^{2-}$	−196.5	51.8
$[UO_2(CO_3)_3]^{4-}$ + R″HAO/HAc → $[UO_2(CO_3)(R″AO/Ac)]^{2-}$ + 2HCO$_3^-$	−349.5	−0.2
$[UO_2(CO_3)_3]^{4-}$ + R″HAO/HAc + 3H$_2$O → UO$_2$(R″AO/Ac)(H$_2$O)$_3$ + 2HCO$_3^-$ + CO$_3^{2-}$	−202.9	51.7
$[UO_2(CO_3)_3]^{4-}$ + R″H$_2$A → $[UO_2(CO_3)(R″HA)]^-$ + HCO$_3^-$ + CO$_3^{2-}$	−200.5	35.6
$[UO_2(CO_3)_3]^{4-}$ + R″H$_2$A + 3H$_2$O → $[UO_2(R″HA)(H_2O)_3]^+$ + HCO$_3^-$ + 2CO$_3^{2-}$	69.5	91.6
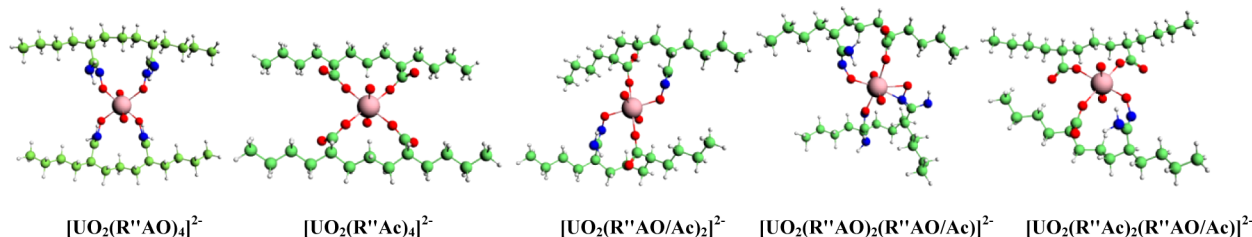
Figure 8. Optimized structures of the charged uranyl complexes with R″AO⁻ and R″Ac⁻ on double alkyl chains (R″=$C_{13}H_{26}$).

and larger WBIs values compared to those of the U−N(R″AO⁻/R″HA⁻) bonds (Supporting Information, Tables S5 and S6), confirming that in these coordination modes, the oxygen atoms show much stronger coordinating ability to the metal atoms. Additionally, the very low net charges on uranium atoms indicate the important electronic charge transfer from the ligands toward the metal atoms.

Tables 6 and 7 list a series of possible extration reactions with $[UO_2(CO_3)_3]^{4-}$ as reactant. From our calculations, the ΔG_g values are all negative, while the energetics are strongly endothermic by taking into account solvent effects. Thus, our results suggest that these reactions do not seem to occur at room temperature in aqueous solution, which can be expected since most of the single chain binding reactions are endothermic in solution. Nevertheless, the calculated results reported here can predict the stability trends of these uranyl extraction complexes. As shown in Table 6, $[UO_2(R′Ac)_4]^{2-}$ are energetically more stable than other species. Nevertheless, it is obviously observed that all the charged species with mixed ligands R″AO/Ac are more stable than those of the corresponding species with single

R″AO ligands. For the neutral complexes (Table 7), the reaction energies with UO$_2$(R″HAO/Ac)$_2$ and UO$_2$(R″HAc/AO)$_2$ are lower than the corresponding reaction with UO$_2$(R″HAO/AO)$_2$ and UO$_2$(R″HAc/Ac)$_2$. These results indicate that introdution of Ac groups can increase the uranium adsorption capacity. Note that species with R″HAO/Ac are more stable than those with R″AO/HAc, and UO$_2$(R″HAO/Ac)$_2$ seems to be the most stable species, mainly due to higher ability of R′HAc to release hydrogen ions. Moreover, UO$_2$(R″HA)$_2$ seems to be more stable than UO$_2$(R″HAO/Ac)$_2$, and the advantage of the R″HA⁻/Ac⁻ groups in the complexes of UO$_2$(R″HA/Ac) was also observed. This indicates that adsorbents with tridentate R″HA⁻ ligand have stronger coordination abiliy, which is in agreement with experimental predictions.[14−16] Since R″HAc groups on alkyl chains (R″=$C_{13}H_{26}$) are more easily decomposed compared to R″H$_2$A, we can thus deduce that adsorbents with a tridentate R″HA⁻ ligand have stronger coordination abiliy than those with a bidentate R″Ac⁻ ligand.

UO$_2$(R''HAO/AO)$_2$ **UO$_2$(R''HAc/Ac)$_2$** **UO$_2$(R''HAO/AO)(R''HAc/Ac)** **UO$_2$(R''HAO/Ac)$_2$**

UO$_2$(R''HAc/AO)$_2$ **UO$_2$(R''AO/HAc)(R''HAO/AO)** **UO$_2$(R''HAO/Ac)(R''AO/HAO)** **UO$_2$(R''HAO/Ac)(R''Ac/HAc)**

UO$_2$(R''HAc/Ac)(R''AO/HAc) **UO$_2$(R''HA)$_2$** **UO$_2$(R''HA)(R''Ac)**
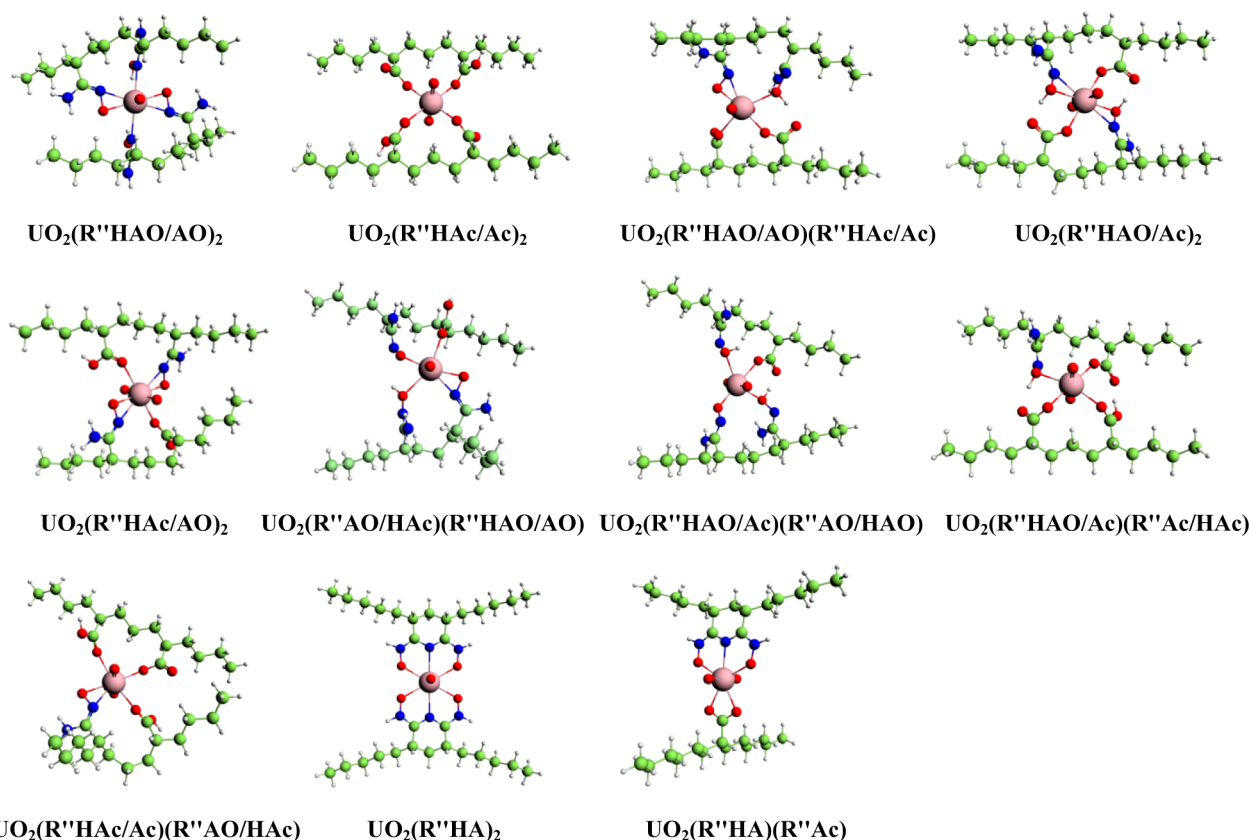
Figure 9. Optimized structures of the neutral uranyl complexes with R''AO$^-$, R''Ac$^-$, and R''HA$^-$ on double alkyl chains (R''=C$_{13}$H$_{26}$).

Table 6. Changes of the Gibbs Free Energy (kcal/mol) for Reactions of Forming Charged Uranyl Complexes with R''AO$^-$ and R''Ac$^-$ on Double Alkyl Chains (R''=C$_{13}$H$_{26}$) in the Gas Phase and Aqueous Solution

reactions	ΔG_g	ΔG_{sol}
$[UO_2(CO_3)_3]^{4-} + 2(R''HAO)_2 + H_2O \rightarrow [UO_2(R''AO)_4]^{2-} + 3HCO_3^- + H_3O^+$	−149.5	36.1
$[UO_2(CO_3)_3]^{4-} + 2(R''HAc)_2 + H_2O \rightarrow [UO_2(R''Ac)_4]^{2-} + 3HCO_3^- + H_3O^+$	−196.8	11.0
$[UO_2(CO_3)_3]^{4-} + 2(R''HAO/HAc) + H_2O \rightarrow [UO_2(R''AO/Ac)_2]^{2-} + 3HCO_3^- + H_3O^+$	−185.7	24.9
$[UO_2(CO_3)_3]^{4-} + (R''HAO)_2 + (R''HAO/HAc) + H_2O \rightarrow [UO_2(R''AO)_2(R''AO/Ac)]^{2-} + 3HCO_3^- + H_3O^+$	−163.2	33.5
$[UO_2(CO_3)_3]^{4-} + (R''HAc)_2 + (R''HAO/HAc) + H_2O \rightarrow [UO_2(R''Ac)_2(R''AO/Ac)]^{2-} + 3HCO_3^- + H_3O^+$	−191.3	20.6

Table 7. Changes of the Gibbs Free Energy (kcal/mol) for Reactions of Forming Neutral Uranyl Complexes with R''AO$^-$, R''Ac$^-$, and R''HA$^-$ on Double Alkyl Chains (R''=C$_{13}$H$_{26}$) in the Gas Phase and Aqueous Solution

reactions	ΔG_g	ΔG_{sol}
$[UO_2(CO_3)_3]^{4-} + 2(R''HAO/HAO) \rightarrow UO_2(R''HAO/AO)_2 + 2HCO_3^- + CO_3^{2-}$	−202.6	45.9
$[UO_2(CO_3)_3]^{4-} + 2(R''HAc/HAc) \rightarrow UO_2(R''HAc/Ac)_2 + 2HCO_3^- + CO_3^{2-}$	−166.6	67.3
$[UO_2(CO_3)_3]^{4-} + (R''HAO/HAO) + (R''HAc/HAc) \rightarrow UO_2(R''HAO/AO)(R''HAc/Ac) + 2HCO_3^- + CO_3^{2-}$	−181.7	61.4
$[UO_2(CO_3)_3]^{4-} + 2(R''HAO/HAc) \rightarrow UO_2(R''HAO/Ac)_2 + 2HCO_3^- + CO_3^{2-}$	−204.4	44.4
$[UO_2(CO_3)_3]^{4-} + 2(R''HAO/HAc) \rightarrow UO_2(R''HAc/AO)_2 + 2HCO_3^- + CO_3^{2-}$	−174.4	61.9
$[UO_2(CO_3)_3]^{4-} + (R''HAO/HAc) + (R''HAO/HAO) \rightarrow UO_2(R''AO/HAc)(R''HAO/AO) + 2HCO_3^- + CO_3^{2-}$	−175.5	63.4
$[UO_2(CO_3)_3]^{4-} + (R''HAO/HAc) + (R''HAO/HAO) \rightarrow UO_2(R''HAO/Ac)(R''AO/HAO) + 2HCO_3^- + CO_3^{2-}$	−185.5	58.8
$[UO_2(CO_3)_3]^{4-} + (R''HAO/HAc) + (R''HAc/HAc) \rightarrow UO_2(R''HAO/Ac)(R''Ac/HAc) + 2HCO_3^- + CO_3^{2-}$	−201.5	49.7
$[UO_2(CO_3)_3]^{4-} + (R''HAc/HAc) + (R''HAO/HAc) \rightarrow UO_2(R''HAc/Ac)(R''AO/HAc) + 2HCO_3^- + CO_3^{2-}$	−171.5	64.1
$[UO_2(CO_3)_3]^{4-} + 2 (R''H_2A) \rightarrow UO_2(R''HA)_2 + 2HCO_3^- + CO_3^{2-}$	−176.2	41.0
$[UO_2(CO_3)_3]^{4-} + (R''H_2A) + (R''HAc) \rightarrow UO_2(R''HA)(R''Ac) + 2HCO_3^- + CO_3^{2-}$	−194.9	38.9

4. CONCLUSIONS

In this work, DFT methods were used to study the equilibrium geometrical structures, electronic structures, and thermodynamic stabilities of various uranyl complexes. Two alkyl chains (R'= CH$_3$, R''=C$_{13}$H$_{26}$) with amidoxime (AO$^-$), carboxyl (Ac$^-$), glutarimidedioxime (HA$^-$), and AO$^-$/Ac$^-$, HA$^-$/Ac$^-$ groups have been considered as sorbents used in uranium extraction. The AO$^-$ and Ac$^-$ groups coordinate as monodentate and bidentate ligands to the uranyl cations, while HA$^-$ are tridentate ligands. For complexing species with AO$^-$ groups in η^2 mode, the bond lengths between the uranium and oxygen atoms U— O(AO$^-$) are shorter compared to those between uranium and

nitrogen atoms U−N(AO⁻). Besides, U−O(AO⁻) bonds show larger WBIs values, suggesting that the oxime oxygen atoms have stronger coordination ability to uranyl than the nitrogen atom. In complexes with mixed ligands AO⁻/Ac⁻ and HA⁻/Ac⁻, HA⁻ exhibits the highest ligand-to-metal charge transfer among the studied ligands, while Ac⁻ has the lowest charge transfer, implying the stronger interaction between HA⁻ and uranyl cations.

The reaction kinetic analysis for the model reaction of $[UO_2(CO_3)_3]^{4-} + R'HAO \rightarrow [UO_2(CO_3)_2(R'AO)]^{3-} + HCO_3^-$ found that the rate-determining step is the dissociation of the carbonate group accompanying with the complexation of uranyl and amidoxime ligand. According to thermodynamic analysis, the metal−ligand complexing reactions can easily proceed in the gas phase and aqueous solution, and species with AO⁻ groups are more stable than those with Ac⁻ groups in terms of the calculated binding energies. For the possible extraction reactions with $[UO_2(CO_3)_3]^{4-}$ as the reactant, most of these reactions are endothermic in aqueous solution and do not appear to occur in solution based on theoretical calculations with predicted reactions. However, comparing the values of the calculated reaction energies, the Ac⁻ groups seem more efficient for uranium recovery compared to AO⁻ because the HAc groups are much easier to decompose than HAO. Additionally, compared to the AO⁻ and Ac⁻ groups, the HA⁻ groups are more favorable for binding with uranyl ions due to their tridentate feature. Furthermore, the complexing species with mixed ligands AO⁻/Ac⁻ and HA⁻/Ac⁻ are more thermodynamically favorable than those with monoligands AO⁻ or HA⁻, confirming that the coexistence of amidoxime and carboxyl groups can enhance the adsorbability of uranium.

In all, this study systematically explored the coordination modes and bonding natures of possible uranium complexes associated with uranium extraction from seawater. Besides giving valuable theoretical explanations for previous experimental efforts, our results can provide more insights for designing highly efficient agents for uranium recovery from seawater.

■ ASSOCIATED CONTENT

Ⓢ Supporting Information

Optimized structures of $UO_2(R'AO)_2(MeOH)_2$ (R′=CH₃) and $UO_2(HA)_2$; optimized structures and total energies after zero-point energy correction (in hartrees) of uranyl complexes with R′AO⁻, R′Ac⁻, R′₂HA⁻ (R=CH₃), and CO_3^{2-} by the B3LYP method; optimized structures and total energies after zero-point energy correction (in hartrees) of uranyl complexes with R″AO⁻, R″Ac⁻, and R″HA⁻ on a single alkyl chain (R″= C₁₃H₂₆) by the B3LYP method; optimized structures and total energies after zero-point energy correction (in hartrees) of uranyl complexes with R″AO⁻, R″Ac⁻, and R″HA⁻ on double alkyl chains (R″=C₁₃H₂₆) by the B3LYP method; the U−O(R′AO) (R′=CH₃) π-bonding in the uranyl complexes; NBO σ and π orbitals of the U−O(R′AO) bonds, and NBO σ orbitals of the U−O(R′Ac), U−O(R′₂HA), and U−N(R′₂HA) bonds in the uranyl complexes; tabulated data indicating selected average bond lengths (Å) for $UO_2(R'AO)_2(MeOH)_2$ (R′=CH₃) and $UO_2(HA)_2$ calculated by the B3LYP method in comparison with previous theoretical data (in parentheses) and available experimental data; the changes of Gibbs energy (kcal/mol) for the reactions of uranyl complexes with R′AO⁻ and R′₂HA⁻ in aqueous solution at temperatures of 100, 200, 300, and 400 K; the U−N and U−O average bond lengths (Å) for the uranyl complexes with R″AO⁻, R″Ac⁻, and R″HA⁻ on a single alkyl

chain (R″=C₁₃H₂₆), the symmetrical and antisymmetrical stretching frequency (v_s and v_{as}, cm⁻¹) of U=O(axial), the Wiberg bond indices (WBIs) of U−N and U−O bonds and natural charges on the U, N, and O atoms by the B3LYP method; the U−N and U−O average bond lengths (Å) for the charged and neutral uranyl complexes with R″AO⁻, R″Ac⁻, and R″HA⁻ on double alkyl chains, the Wiberg bond indices (WBIs) of U−N and U−O bonds, and natural charges on the U atoms by the B3LYP method. This material is available free of charge via the Internet at http://pubs.acs.org.

■ AUTHOR INFORMATION

Corresponding Authors

*E-mail: shiwq@ihep.ac.cn. (W.-Q.S.)
*E-mail: zfchai@suda.edu.cn. (Z.-F.C.)

Notes

The authors declare no competing financial interest.

■ REFERENCES

(1) Davies, R. V.; Kennedy, J.; McIlroy, R. W.; Spence, R.; Hill, K. M. *Nature* **1964**, *203*, 1110.

(2) Schenk, H. J.; Astheimer, L.; Witte, E. G.; Schwochau, K. *Sep. Sci. Technol.* **1982**, *17*, 1293.

(3) Scanlan, J. P. *J. Inorg. Nucl. Chem.* **1977**, *39*, 635.

(4) Choppin, G. R. *Mar. Chem.* **1989**, *28*, 19.

(5) Vernon, F.; Shah, T. *React. Polym.* **1983**, *1*, 301.

(6) Omichi, H.; Katakai, A.; Sugo, T.; Okamoto, J. *Sep. Sci. Technol.* **1986**, *21*, 563.

(7) Kabay, N. *Sep. Sci. Technol.* **1994**, *29*, 375.

(8) Sekiguchi, K.; Serizawa, K.; Konishi, S.; Saito, K.; Furusaki, S.; Sugo, T. *React. Polym.* **1994**, *23*, 141.

(9) Katragadda, S.; Gesser, H. D.; Chow, A. *Talanta* **1997**, *45*, 257.

(10) Sahiner, N.; Pekel, N.; Akkas, P.; Guven, O. *J. M. S. Pure Appl. Chem. A* **2000**, *37*, 1159.

(11) Seko, N.; Katakai, A.; Hasegawa, S.; Tamada, M.; Kasai, N.; Takeda, H.; Sugo, T.; Saito, K. *Nucl. Technol.* **2003**, *144*, 274.

(12) Seko, N.; Katakai, A.; Tamada, M.; Sugo, T.; Yoshii, F. *Sep. Sci. Technol.* **2005**, *29*, 3753.

(13) Vukovic, S.; Watson, L.; Kang, S. O.; Custelcean, R.; Hay, B. P. *Inorg. Chem.* **2012**, *51*, 3855.

(14) Astheimer, L.; Schenk, H. J.; Witte, E. G.; Schwochau, K. *Sep. Sci. Technol.* **1983**, *18*, 307.

(15) Kang, S. O.; Vukovic, S.; Custelcean, R.; Hay, B. P. *Ind. Eng. Chem. Res.* **2012**, *51*, 6619.

(16) Tian, G.; Teat, S. J.; Zhang, Z.; Rao, L. *Dalton Trans.* **2012**, *41*, 11579.

(17) Kim, J.; Tsouris, C.; Mayes, R. T.; Oyola, Y.; Saito, T.; Janke, C. J.; Dai, S.; Schneider, E.; Sachde, D. *Sep. Sci. Technol.* **2013**, *48*, 367.

(18) Das, S.; Pandey, A. K.; Athawale, A.; Kumar, V.; Bhardwaj, Y. K.; Sabharwal, S.; Manchanda, V. K. *Desalination* **2008**, *232*, 243.

(19) Das, S.; Pandey, A. K.; Athawale, A. A.; Manchanda, V. K. *J. Phys. Chem. B* **2009**, *113*, 6328.

(20) Omichi, H.; Katakai, A.; Sugo, T.; Okamoto, J. *Sep. Sci. Technol.* **1986**, *21*, 299.

(21) Kawai, T.; Saito, K.; Sugita, K.; Katakai, A.; Seko, N.; Sugo, T.; Kanno, J.-i.; Kawakami, T. *Ind. Eng. Chem. Res.* **2000**, *39*, 2910.

(22) Choi, S.-H.; Choi, M.-S.; Park, Y.-T.; Lee, K.-P.; Kang, H.-D. *Radiat. Phys. Chem.* **2003**, *67*, 387.

(23) Choi, S.-H.; Nho, Y. C. *Radiat. Phys. Chem.* **2000**, *57*, 187.

(24) Sekiguchi, K.; Saito, K.; Konishi, S.; Furusaki, S.; Sugo, T.; Nobukawa, H. *Ind. Eng. Chem. Res.* **1994**, *33*, 662.

(25) Vukovic, S.; Hay, B. P. *Inorg. Chem.* **2013**, *52*, 7805.

(26) Xu, C. F.; Su, J.; Xu, X.; Li, J. *Sci. China: Chem.* **2013**, *56*, 1525.

(27) Abney, C. W.; Liu, S.; Lin, W. *J. Phys. Chem. A* **2013**, *117*, 11558.

(28) Frisch, M. J.; Trucks, G. W.; Schlegel, H. B.; Scuseria, G. E.; Robb, M. A.; Cheeseman, J. R.; Montgomery, Jr., J. A.; Vreven, T.; Kudin, K. N.; Burant, J. C.; Millam, J. M.; Iyengar, S. S.; Tomasi, J.; Barone, V.; Mennucci, B.; Cossi, M.; Scalmani, G.; Rega, N.; Petersson, G. A.; Nakatsuji, H.; Hada, M.; Ehara, M.; Toyota, K.; Fukuda, R.; Hasegawa, J.; Ishida, M.; Nakajima, T.; Honda, Y.; Kitao, O.; Nakai, H.; Klene, M.; Li, X.; Knox, J. E.; Hratchian, H. P.; Cross, J. B.; Bakken, V.; Adamo, C.; Jaramillo, J.; Gomperts, R.; Stratmann, R. E.; Yazyev, O.; Austin, A. J.; Cammi, R.; Pomelli, C.; Ochterski, J. W.; Ayala, P. Y.; Morokuma, K.; Voth, G. A.; Salvador, P.; Dannenberg, J. J.; Zakrzewski, V. G.; Dapprich, S.; Daniels, A. D.; Strain, M. C.; Farkas, O.; Malick, D. K.; Rabuck, A. D.; Raghavachari, K.; Foresman, J. B.; Ortiz, J. V.; Cui, Q.; Baboul, A. G.; Clifford, S.; Cioslowski, J.; Stefanov, B. B.; Liu, G.; Liashenko, A.; Piskorz, P.; Komaromi, I.; Martin, R. L.; Fox, D. J.; Keith, T.; Al-Laham, M. A.; Peng, C. Y.; Nanayakkara, A.; Challacombe, M.; Gill, P. M. W.; Johnson, B.; Chen, W.; Wong, M. W.; Gonzalez, C.; Pople, J. A. *Gaussian 09, Revision A.02*; Gaussian, Inc.: Wallingford, CT, 2009.

(29) Ehlers, A. W.; Frenking, G. *J. Am. Chem. Soc.* **1994**, *116*, 1514.

(30) Delly, B.; Wrinn, M.; Lüthi, H. P. *J. Chem. Phys.* **1994**, *100*, 5785.

(31) Li, J.; Schreckenbach, G.; Ziegler, T. *J. Am. Chem. Soc.* **1995**, *117*, 486.

(32) Jonas, V.; Thiel, W. *J. Chem. Phys.* **1995**, *102*, 8474.

(33) Becke, A. D. *J. Chem. Phys.* **1993**, *98*, 5648.

(34) Lee, C.; Yang, W.; Parr, R. G. *Phys. Rev. B* **1988**, *37*, 785.

(35) Kuchle, W.; Dolg, M.; Stoll, H.; Preuss, H. *J. Chem. Phys.* **1994**, *100*, 7535.

(36) Cao, X.; Dolg, M. *J. Mol. Struct.: THEOCHEM* **2004**, *673*, 203.

(37) Cao, X.; Dolg, M. *J. Mol. Struct.: THEOCHEM* **2002**, *581*, 139.

(38) Lan, J. H.; Shi, W. Q.; Yuan, L. Y.; Zhao, Y. L.; Li, J.; Chai, Z. F. *Inorg. Chem.* **2011**, *50*, 9230.

(39) Lan, J. H.; Shi, W. Q.; Yuan, L. Y.; Feng, Y. X.; Zhao, Y. L.; Chai, Z. F. *J. Phys. Chem. A* **2012**, *116*, 504.

(40) Lan, J. H.; Shi, W. Q.; Yuan, L. Y.; Li, J.; Zhao, Y. L.; Chai, Z. F. *Coord. Chem. Rev.* **2012**, *256*, 1406.

(41) Wang, C. Z.; Lan, J. H.; Zhao, Y. L.; Chai, Z. F.; Wei, Y.-Z.; Shi, W. Q. *Inorg. Chem.* **2013**, *52*, 196.

(42) Wang, C. Z.; Shi, W. Q.; Lan, J. H.; Zhao, Y. L.; Wei, Y.-Z.; Chai, Z. F. *Inorg. Chem.* **2013**, *52*, 10904.

(43) Klamt, A.; Schüürmann, G. *J. Chem. Soc., Perkin Trans.* **1993**, *2*, 799.

(44) Andzelm, J.; Kölmel, C.; Klamt, A. *J. Chem. Phys.* **1995**, *103*, 9312.

(45) Barone, V.; Cossi, M. *J. Phys. Chem. A* **1998**, *102*, 1995.

(46) Cossi, M.; Rega, N.; Scalmani, G.; Barone, V. *J. Comput. Chem.* **2003**, *24*, 669.

(47) Pliego, J. R.; Riveros, J. M. *Chem. Phys. Lett.* **2000**, *332*, 597.

(48) Camaioni, D. M.; Schwerdtfeger, C. A. *J. Phys. Chem. A* **2005**, *109*, 10795.

(49) Shamov, G. A.; Schreckenbach, G. *J. Phys. Chem. A* **2005**, *109*, 10961. Correction note: Shamov, G. A.; Schreckenbach, G. *J. Phys. Chem. A* **2006**, *110*, 12072.

(50) Shamov, G. A.; Schreckenbach, G.; Martin, R. L.; Hay, P. J. *Inorg. Chem.* **2008**, *47*, 1465.